Lumped Mass Model of a 1D Metastructure for Vibration Suppression with no Additional Mass

Katherine K. Reichl[a,*], Daniel J. Inman[a]

[a] *Department of Aerospace Engineering, University of Michigan, 1320 Beal Ave, Ann Arbor, MI 48109, USA*

*Corresponding Author.
E-mail Address: reichl@umich.edu

Abstract

The article examines the effectiveness of metastructures for vibration suppression from a weight standpoint. Metastructures, a metamaterial inspired concept, are structures with distributed vibration absorbers. In automotive and aerospace industries, it is critical to have low levels of vibrations while also using lightweight materials. Previous work has shown that metastructures are effective at mitigating vibrations, but do not consider the effects of mass. This work takes mass into consideration by comparing a structure with vibration absorbers to a structure of equal mass with no absorbers. These structurers are modeled as one-dimensional lumped mass models, chosen for simplicity. Results compare both the steady-state and the transient responses. As a quantitative performance measure, the H_2 norm, which is related to the area under the frequency response function, is calculated and compared for both the metastructure and the baseline structure. These results show that it is possible to obtain a favorable vibration response without adding additional mass to the structure. Additionally, the performance measure is utilized to optimize the geometry of the structure, determine the optimal ratio of mass in the absorber to mass of the host structure, and determine the frequencies of the absorbers. The trends from this model are replicated using previous experimental results.

Keywords: vibration suppression, metastructure, passive damping

1. Introduction

Metastructures are a metamaterial inspired concept. Metamaterial research began by investigating electromagnetic metamaterials which exhibited a negative permittivity and or permeability [1,2]. Inspired by the electromagnetic metamaterials, the concepts were extended to acoustic metamaterials [3]. Traditional metamaterials utilize the theory of Bragg scattering. The lattices are created such that when the waves reflect off the structure, they destructively interfere with each other. In order for the Bragg scattering mechanism to work, the periodic length of the material must be of similar length as the

wavelength. Thus, for low frequencies very large structures are required [4]. Metamaterials that rely on the Bragg scattering mechanism are commonly called phononic crystals. Phononic crystals are materials which exhibit some type of periodicity and are reviewed in a paper by Hussein *et al* [5]. Milton and Willis were the first to conceive the idea of using local absorbers to create structures with negative effective mass that varies with frequency [6]. Liu *et al* created the first physical metastructure that was able to create a bandgap at a frequency lower than that of the Bragg scattering mechanism. This structure is designed to suppress acoustic waves above 300 Hz. Their acoustic metamaterial contains lead spheres coated in a silicone rubber within an epoxy matrix. The lead balls in the rubber are referred to as local resonators. The local resonator mechanism is the same mechanism used for vibration suppression [7]. Since then locally resonant metamaterials have been studied extensively for both acoustic and vibration isolation applications. The work presented here deals exclusively with vibration mitigation applications. Structures or materials capable of suppressing vibrations using these local resonators are often referred to as elastic metamaterials. In a review paper by Zhu *et el*, the authors provide a review of various type of plate-type elastic metamaterials and discuss possible applications. They also provide an explanation of the negative mass density and negative bulk modulus [8]. Here the term *metastructure* is used to refer to structures with distributed vibration absorbers. These structures use conventional materials with absorbers integrated into the structure through geometry and material changes on the centimeter scale. The periodic-type nature of these structures was inspired from metamaterials but the larger scale modifications makes the term structure a more fitting term for this work. In the literature, these are also referred to as locally resonant phononic crystals or elastic metamaterials. The field of auxetics also has considerable overlap with metastructures. Auxetics are materials that exhibit a negative Poisson's ratio. These materials are realized by creating periodic lattice structures. Because of the periodic nature of auxetics, they affect how waves propagate through them and thus can be used for vibration suppression among other applications [9].

As Hussein *et al* describes in his review paper, metastructures are at the cross roads of vibration and acoustics engineering, and condensed matter physics [5]. Thus, it is important that strengths from both fields are considered and reviewed for relevancy. Sun *et al* and Pai looked into the working mechanism of metastructures for both bending and longitudinal motion. They were able to conclude that the working mechanism that leads to vibration suppression is based on the concept of mechanical vibration absorbers that do not need to be small or closely spaced [10,11]. Therefore, it is also relevant to explore the literature regarding vibration absorbers. Vibration absorbers can also be called tuned mass dampers (TMDs) or dynamic vibration absorbers. TMDs typically consist of mass-spring-damper systems, while a vibration absorber does not use a damper to add significant localized damping. Although there is no

localized damper added to the vibration absorber, there is still a small amount of material damping which is inherent in all structures. TMDs are studied widely in the field of earthquake engineering. Igusa and Xu were the first researchers to look at the effects of using multiple (TMDs) to suppress a single mode of a structure [12,13]. Later, this was also studied by Yamaguchi and Harnprnchai [14]. Their work focuses on attaching multiple TMDs to a single degree of freedom system and shows that multiple TMDs can be more effective than a single TMD. These results can be leveraged in metastructure research.

Another important aspect of the TMD literature is how the optimal parameters for the TMDs were determined. Many methods have been used and applied to various systems. DenHartog developed the optimal parameters for a single TMD as an analytical expression [15] and this result has since been studied by many others as summarized in Sun *et al*'s review paper [16]. The work presented here focuses on some of the numerical methods utilized by many TMD researchers specifically the H_2 norm. Parameters are chosen such that the H_2 norm is minimized. This performance metric describes the response of a structure excited across all frequencies [17,18]. The H_2 norm provides different results than those obtained by suppressing a specific frequency range and tend to suppress the fundamental mode which typically has the largest magnitude response.

The model used in this paper is a one-dimensional lumped mass model, which was chosen for its simplicity, and allows the dynamics to be understood more thoroughly. Some of the most relevant work related to 1D metastructures is from Pai who models a longitudinal metastructure consisting of a hollow tube with many small mass-spring systems distributed throughout the bar. He suggests that the ideal design for a metastructure, involves absorbers with varying tuned frequencies [11]. Xiao *et al* looks at a similar structure as Pai but considers multiple degree of freedom resonators. Their work focuses on modeling procedures and understanding the bandgap formation mechanisms [19]. The favorable dynamics response of these structures can also be described as having a negative effective mass which has been shown analytically and experimentally [6,20,21]. In addition, other researchers have conducted experiments on longitudinal metastructures. Zhu *et al* looked at a thin plate with cantilever absorbers cut out of the plate. They were able to show the ability to accurately predict the band-gap and also compared various absorber designs [22]. Wang *et al* tested a glass bar with cantilever absorbers made out of steel slices and a mass [23]. With the rise in additive manufacturing, 3D printing has become a good method to realize the complex geometry needed for these structures [24]. Hobeck *et al* and Nobrega *et al* both created longitudinal 3D metastructures and obtained experimental results. Hobeck *et al*'s work will be discussed in detail later [25,26].

In this paper, the feasibility of adding distributed vibration absorbers to a structure without increasing the overall weight of the structure is presented. When creating these metastructures, much of the previous work looks at keeping the stiffness constant, which requires adding additional mass to the structure [27–29]. Taking an alternative approach, this paper keeps the mass constant by redistributing mass from the host structure to the distributed absorber system. Mass and suppression properties are inherently tied together which motivates this approach. Simply adding mass to a structure will result in increased suppression. It is important to isolate the effects of the dynamics of the vibration absorbers from the added mass. It must be shown that the additional mass is not causing the increased performance. Since a lumped mass model is used, the redistribution of mass does not affect the stiffness of the structure. In real structure where mass and stiffness are coupled, the stiffness would be affected. Other researchers have looked at constant stiffness structures but haven't shown if the additional mass or the dynamics of the absorbers are causing the increased performance. By using a mass constant constraint, this work shows that the vibration absorber dynamics, and not the additional mass, are increasing the suppression. Additionally in both automotive and aerospace structures, it is critical to keep the total weight of the structure low.. The strategy taken here is to model a discrete system undergoing axial vibrations. This is used as a starting point because the analysis for a unidirectional discrete problem is relatively straight-forward and enables understanding of the basic issues and phenomenon. The model consists of masses and springs connected in series with an absorber attached to each one of the masses. The mass and stiffness of these components are varied in order to get the desired dynamics. Material damping inherent in all structures is represented by a proportional damping model and is added to this model such the simulations do not go to infinity. The metastructure described here is compared to a baseline structure which has no vibration absorbers, which illustrates that the favorable damping comes from the addition of the distributed vibration absorbers and not from adding mass to the system. The focus of the vibration suppression is on the fundamental natural frequency of the structure as opposed to creating a band-gap at higher frequencies, which much of the metamaterial research examines. In engineering applications, it is important to suppress the frequencies near the fundamental mode of vibration, as these frequencies typically result in the highest magnitude response. A similar approach is taken when designing TMDs, explaining the motivation for using performance metrics from the TMD literature.

The work of Igusa and Xu is similar to the work presented here but there are some important differences. They are comparing the effectiveness of a single TMD and multiple TMDs whereas this work compares multiple vibration absorbers to no absorbers. Thus their structure with vibration suppression is heavier than their structure without suppression. In this work the suppression system does not add weight to the structure. Additionally, Igusa and Xu use TMDs so they can tune the mass, stiffness and damping of each

absorber [13]. The work presented here does not add dampers with high levels of localized damping to the vibration absorbers, thus only mass and stiffness can be tuned.

The methodology used for this paper begins by introducing the model used and the parameters that characterize this model. The main parameters varied throughout this study are the number of absorbers, the mass ratio (ratio of absorber mass to mass of the rest of the structure), and the natural frequencies of the individual absorbers. Other variables in the model are calculated such that the mass of the structure is constant and the fundamental frequency of the entire structure stays relatively constant throughout the analysis. Both steady state and transient responses are examined. Next, the analysis of the model is described and details about the performance measures are provided. These are the H_2 and H_∞ norms, which measure the total energy of the system and the maximum response respectively. An optimization procedure is set up to minimize the H_2 norm and shows the trade-offs between various parameters. All of the metastructure models created are compared to a baseline structure which has equal mass but no distributed vibration absorbers. The constant mass means any increase in performance can be attributed to the addition of the absorbers. Lastly, the simulation results will be compared to experimental data, from work completed by Hobeck *et al*, to show that trends found from this longitudinal model match the trends found from their experimental data [25].

2. Lumped Mass Model

Consider the lumped mass model shown in Fig. 1(a) which represents a metastructure bar. This model consists of masses and springs connected in series and all the deformation occurs in the horizontal direction. The model contains the host structure with vibration absorbers distributed along the length of the bar. The larger masses and springs make up the host structure while the smaller masses and springs represent the vibration absorbers. Small deformation is desired in the host structure. To provide a basis for performance improvement, the results for the metastructure are compared to a baseline structure. A simple uniform bar is utilized as the baseline structure and is modeled as mass and springs connected in series, seen in Fig. 1(b). The baseline structure and the metastructure have the same mass, which shows that better performance from the metastructure is due to the addition of the absorbers and not from the additional mass. Throughout this paper, the bars and absorbers are modeled as lumped mass systems so the dynamics of the system are easily understood and computational time is small.

(a) **Metastructure :** Vibration Absorbers

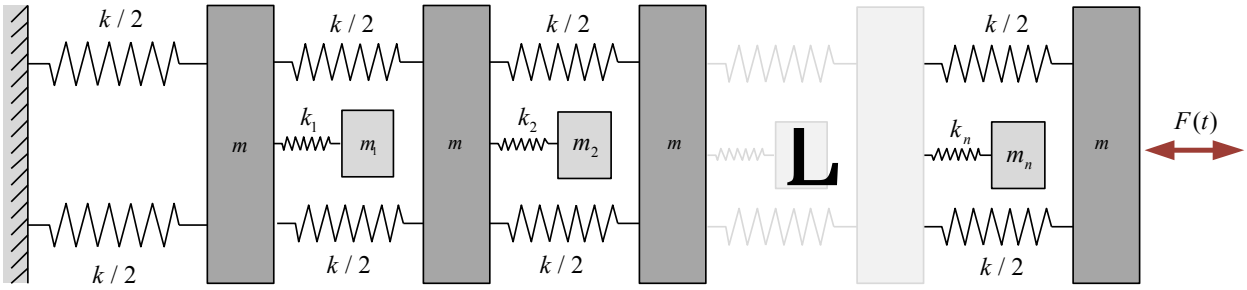

(b) **Baseline Structure :** No Vibration Absorbers

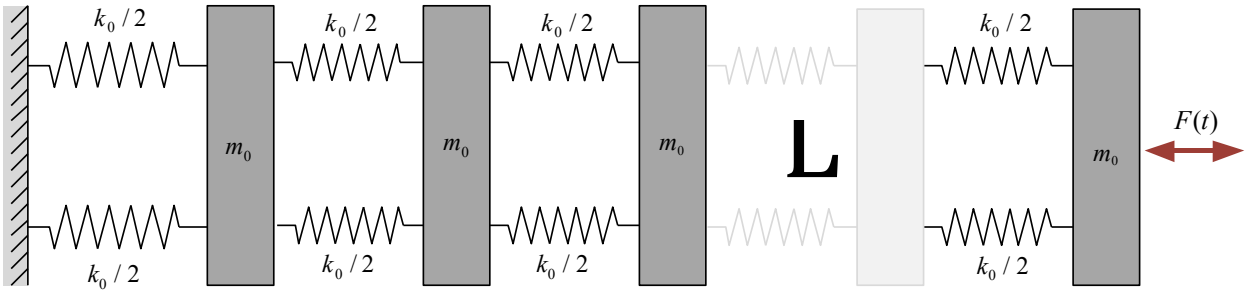

Fig. 1. Lumped mass models of (a) the metastructure and (b) the baseline structure

The design of these structures was chosen such that the dynamics of structures will be comparable between the metastructure and the baseline structure. Most importantly, they will have fundamental natural frequencies near each other. The metastructure is characterized by the number of absorbers it has, denoted n. Therefore, $n + 1$ masses make up the host structure. All masses in the host structure, except the far right mass, have a small absorber connected to it, modeled as a mass and spring. The larger masses will be referred to as the host masses since these make up the host structure whereas the smaller masses are called the absorber masses. The host masses all have the same mass to represent a uniform bar but the mass of the absorbers is allowed to vary throughout the structure. These masses have values of m and m_i respectively where the i refers to the ith absorber mass from the left and ranges from 1 to n. The springs connecting the host masses are called the host springs and are denoted k. The mass ratio, μ is the ratio of the mass of the absorber system to the mass in the host structure, and is calculated by

$$\mu = \frac{\sum_{i=1}^{n} m_i}{(n+1)m} \tag{1}$$

The baseline structure has the same number of masses at the host structure, $N = n + 1$. The mass of each one of these masses, m is calculated by taking the total mass of the metastructure divided by the number

of masses. The springs in the baseline structure have the same stiffness as the host springs in the metastructure. For all simulations, structural damping is utilized to approximate the total material damping in the structure.

2.1. Model Parameters

In this section, specific parameters are calculated for the various structures. In order to see the effect of the number of absorbers, n and the mass ratio, μ these parameters must be varied. For ease of comparison, the fundamental natural frequencies of the structures should be approximately equal. For each model, n and μ must be specified, and the rest of the parameters are calculated using the methods described below. In order to achieve relatively constant fundamental frequencies, the mass and stiffness values are chosen based on a continuous uniform fixed-free bar with a rectangular cross section and parameters shown in Table 1. A finite element type approach is used to obtain m and k. This approach results in a relatively constant natural frequency for varying degrees of freedom. The uniform fixed-free bar of length ℓ is discretized into n elements so that the length of each element, ℓ_{element} is calculated as $\ell_{\text{element}} = \ell/n$. The mass and springs values are calculated for the baseline structure as

$$k_0 = \frac{EAn}{\ell}, \qquad m_0 = \frac{m_{\text{total}}}{n+1} \tag{2}$$

where k_0 and m_0 represent the stiffness and mass values for the baseline structure from Fig. 1, and m_{total}, $E, A,$ and ℓ are defined in Table 1. These values fully define the lumped mass baseline structure model. For the lumped mass metastructure model, the value of the host spring stiffness equals the stiffness from the spring in the baseline structure. The mass of the host mass must change in order to keep the mass constant between the two models. To simplify the problem further, the mass of each of the vibration absorbers is chosen to be constant and is calculated using the mass ratio, μ. The parameters of the metastructure model are calculated as

$$\begin{gathered} k = k_0, \qquad m = (1-\mu)\frac{m_{\text{total}}}{n+1} \\ m_i = \mu\frac{m_{\text{total}}}{n} \end{gathered} \tag{3}$$

where k, m, and m_i are the values of the host mass, host stiffness, and absorber masses respectively. The values of the absorber spring constants are calculated based on the desired frequency of the absorbers. All the absorbers can be tuned to a single frequency or each one can be tuned to a unique frequency. Here, the absorbers are tuned to linearly varying frequencies and this range is defined from the minimum and maximum frequencies, $f_{\min}$ and $f_{\max}$. From these defined parameters, the individual spring constants, k_i can be calculated as

$$\Delta f = \frac{f_{\max} - f_{\min}}{n-1}$$
$$k_i = m_i\left(f_{\max} - \Delta f(i-1)\right)^2 \tag{4}$$

where the frequency terms must have units of rad/s. Along with the properties from Table 1, which stay constant throughout this paper, the parameters of the problem can be fully defined for a given number of absorbers and mass ratio.

Table 1
Continuous Bar Parameters

Property	Value
Young's Modulus, E	1890 MPa
Density, ρ	1.19 g/cm^3
Length, ℓ	0.35 m
Cross Sectional Area, A	1.6 cm^2
Total Mass, m_{total}	0.662 kg

2.2. Development of Mass, Stiffness and Damping Matrices

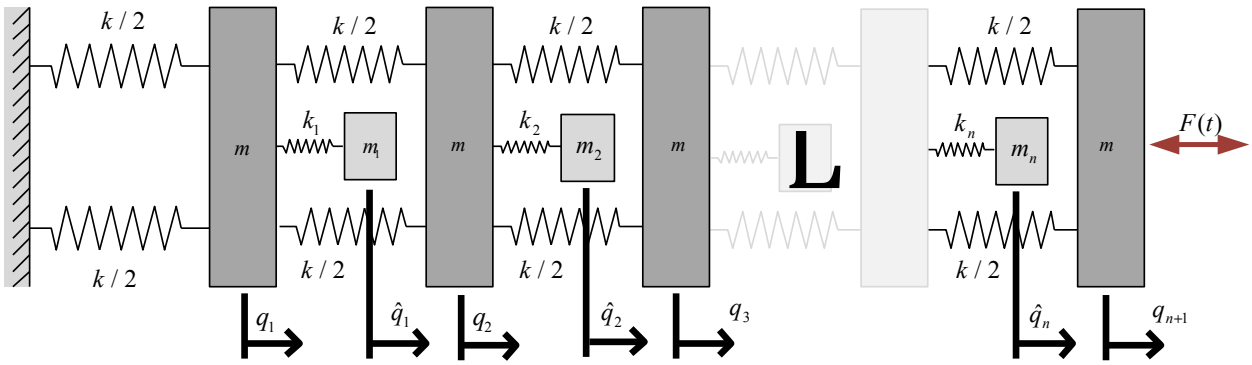

Fig. 2. Definition of mass displacements

Next, the model is assembled into mass, stiffness and damping matrices. The displacements of the masses are defined in Fig. 2. In formulas, the hat refers to displacements of the absorber masses and the subscript refers the absorber number. The individual displacements are arranged into vectors as

$$\begin{aligned} \mathbf{q}_0 &= [q_1^0 \quad q_2^0 \quad \dots \quad q_n^0 \quad q_{n+1}^0]^{\mathrm{T}} \in \mathbb{R}^{(n+1)\times 1} \\ \mathbf{q} &= [q_1 \quad q_2 \quad \dots \quad q_n \quad q_{n+1} \quad \hat{q}_1 \quad \hat{q}_2 \quad \dots \quad \hat{q}_n]^{\mathrm{T}} \in \mathbb{R}^{(2n+1)\times 1} \end{aligned} \tag{5}$$

where the 0 superscript refers to the displacements of the baseline structure masses. Since the structure is a lumped mass model, all the masses are arranged on the diagonal of the global mass matrix. The mass and stiffness matrices are arranged as

$$\begin{aligned} \mathbf{M}_0 &= \mathrm{diag}([m_0 \quad \cdots \quad m_0]) \in \mathbb{R}^{(n+1)\times(n+1)} \\ \mathbf{M} &= \mathrm{diag}([m \quad \cdots \quad m \quad m_1 \quad \cdots \quad m_n]) \in \mathbb{R}^{(2n+1)\times(2n+1)} \end{aligned} \tag{6}$$

$$\mathbf{K}_0 = \begin{bmatrix} 2k & -k & 0 & \cdots & 0 & 0 & 0 \\ -k & 2k & -k & \cdots & 0 & 0 & 0 \\ 0 & -k & 2k & \cdots & 0 & 0 & 0 \\ \vdots & \vdots & \vdots & \ddots & \vdots & \vdots & \vdots \\ 0 & 0 & 0 & \cdots & 2k & -k & 0 \\ 0 & 0 & 0 & \cdots & -k & 2k & -k \\ 0 & 0 & 0 & \cdots & 0 & -k & k \end{bmatrix} \in \mathbb{R}^{(n+1)\times(n+1)} \tag{7}$$

$$\mathbf{K} = \begin{bmatrix} \mathbf{K}_0 + \mathbf{V}_{\text{aug}} & & -\mathbf{V} \\ & & \mathbf{0}^{\text{T}} \\ -\mathbf{V} & \mathbf{0} & \mathbf{V} \end{bmatrix} \in \mathbb{R}^{(2n+1)\times(2n+1)}$$

$$\mathbf{V} = \text{diag}([k_1 \quad k_2 \quad \cdots \quad k_n]) \in \mathbb{R}^{n\times n}$$

$$\mathbf{V}_{aug} = \text{diag}([k_1 \quad k_2 \quad \cdots \quad k_n \quad 0]) \in \mathbb{R}^{(n+1)\times(n+1)}$$

$$\mathbf{0} = [0 \quad \cdots \quad 0]^{\text{T}} \in \mathbb{R}^{n+1}$$

where diag(·) indicates a square matrix with the vector components arranged on the diagonal of the matrix. For this model, no damping is added to the system but since all structures have material damping inherent in them this must be modeled. This damping does not change the dynamics of the system; it simply prevents the simulations from tending to infinity. A proportional damping model is utilized choosing an arbitrary damping constant, α and defining the damping matrices by

$$\begin{aligned} \mathbf{D} &= \alpha\mathbf{K} \\ \mathbf{D}_0 &= \alpha\mathbf{K}_0 \end{aligned} \tag{8}$$

Note that proportionality to the mass matrix, commonly used, is not used here because of the recent result of Kabe and Sako [30]. Results are presented as a pair of plots: the frequency response function (FRF) and the impulse response. Each plot shows the baseline structure with no absorbers as a dotted line and the structure with absorbers as a solid line. The FRF is of the far right main mass subjected to an input force, *i.e.* $\left|Q_{n+1}^0(s)/F_{n+1}(s)\right|$. The impulse response function is also calculated by applying a unit impulse to the same mass. As a quantitative measure, the percent decrease of the H_2 norm is also reported. This norm is explained in more detail in the next section.

3. Performance Measures

This section describes the performance measures used to determine how effectively the structure reduces vibrations. Here the H_2 and the H_∞ norms will be utilized, which are widely used in control literature to develop optimal control theory. The H_2 norm is related to the total energy in the system and the H_∞ norm is related to the maximum energy. To begin, the system must be transformed into state space. The

equations of motion for the structure can be converted into state space and then expressed as a transfer function matrix $\mathbf{H}(s)$ as

$$\mathbf{M}\ddot{\mathbf{q}} + \mathbf{D}\dot{\mathbf{q}} + \mathbf{K}\mathbf{q} = \mathbf{0} \tag{9}$$

$$\mathbf{A} = \begin{bmatrix} \mathbf{0} & \mathbf{I} \\ -\mathbf{M}^{-1}\mathbf{K} & -\mathbf{M}^{-1}\mathbf{D} \end{bmatrix}, \quad \mathbf{B} = \begin{bmatrix} \mathbf{0} \\ -\mathbf{M}^{-1} \end{bmatrix}, \quad \mathbf{C} = [\mathbf{I} \quad \mathbf{0}], \quad \mathbf{D} = [\mathbf{0}] \tag{10}$$

$$\mathbf{H}(s) = \mathbf{C}(s\mathbf{I} - \mathbf{A})^{-1}\mathbf{B} + \mathbf{D} \tag{11}$$

This results in a transfer function matrix, $\mathbf{H}(s)$, which has dimensions $n \times n$ and contains complex numbers. The specific entries of this matrix can be named as

$$\mathbf{H}(s) = \begin{bmatrix} H_{11}(s) & \cdots & H_{1n}(s) \\ \vdots & \ddots & \vdots \\ H_{n1}(s) & \cdots & H_{nn}(s) \end{bmatrix} \tag{12}$$

The term of interest to this paper is the $H_{nn}(s)$ entry which describes the relationship between an input at the tip and the response of the tip. For convenience the following definition is utilized, $H_{nn}(s) = G(s)$. The H_2 norm is a measure of the total vibration energy of the system over all frequencies and can be calculated by taking the norm of frequency response function as follows

$$\|G(s)\|_2^2 = \frac{1}{2\pi}\int_{-\infty}^{\infty} \mathrm{tr}\big(G^{\star}(\mathrm{j}\omega)G(\mathrm{j}\omega)\big)\,\mathrm{d}\omega \tag{13}$$

where the star indicates the complex conjugate of the number. This performance measure is also related to the impulse response function by Parseval's theorem

$$\|G(s)\|_2^2 = \|H(t)\|_2^2 = \int_0^{\infty} h(t)h^T(t)\mathrm{d}t \tag{14}$$

$$h(t) = \mathbf{C}e^{\mathbf{A}t}\mathbf{B} + \delta(t)\mathbf{D} \tag{15}$$

where $h(t)$ is the impulse response function of the system. The H_∞ norm is a measure of the maximum amplitude response, equivalent to looking at the maximum peak of the system in the frequency response plot, and is calculated as

$$\|G(s)\|_\infty = \max_\omega |G(j\omega)| \tag{16}$$

The norms of the metastructure and the baseline structure are compared and presented as a percent decrease in the following section. A larger decrease represents better performance.

4. Simulation Results

Initially, a metastructure model with three main masses, two absorbers, and a mass ratio of $\mu = 0.3$ is examined as shown in **Error! Reference source not found.**. The corresponding baseline structure has a fundamental natural frequency of 766 Hz. The two absorbers in the metastructure are tuned to that same frequency, 766 Hz. Using equations Eq. (3) and (4), m_1 and k_1 are calculated.

The results of this simulation are shown in Fig. 3. The FRF on the left clearly shows that the natural frequency peak of the baseline model gets split into two slightly smaller peaks. If the metastructure system is excited around 766 Hz the response will be minimal but deviation from that excitation frequency will cause in increase in response. This correlates to a 26.0% decrease in the H_2 norm. Looking at the impulse response plot on the right, it is clear that overall, the response of the structure with the absorbers has smaller amplitudes.

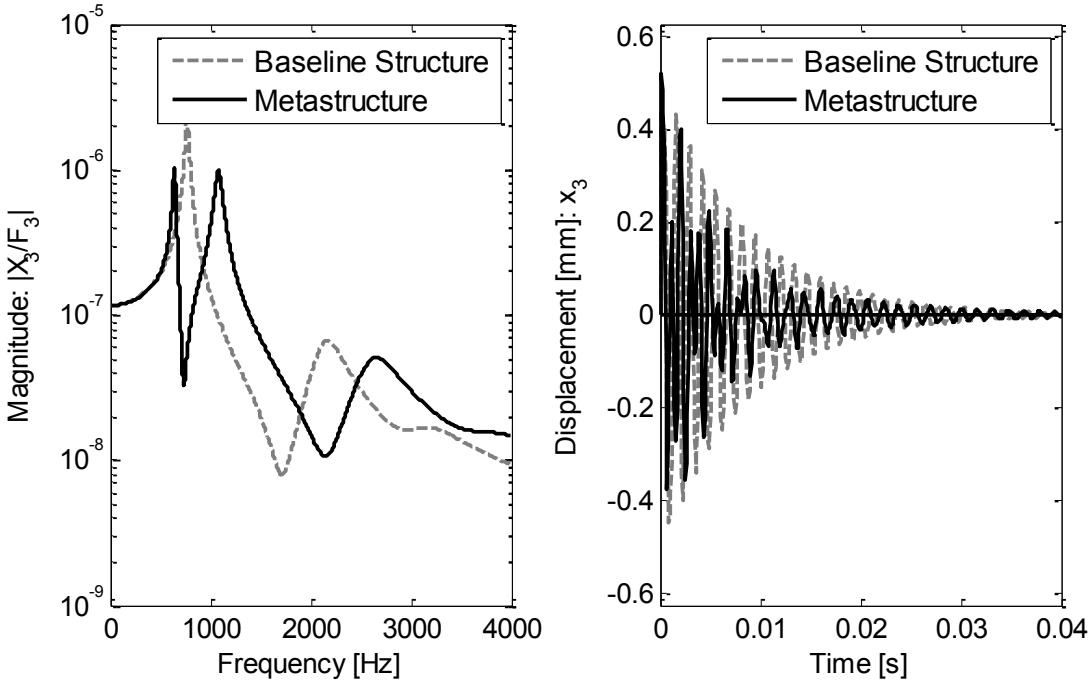

Fig. 3. FRF and the impulse response of two absorbers tuned to the same frequency

The next set of results looks at a system with 20 absorbers. Once again, all the absorbers are tuned to a natural frequency that is equal to the fundamental natural frequency of the baseline structure, which is at 877.2 Hz for this system. This system produces very similar results to the previous system. The H_2 decrease is slightly larger at 27.9%, but overall the trends look the same. This indicates that if all the absorbers are tuned to the same natural frequency, increasing the number of absorbers does not greatly affect the response of the system.

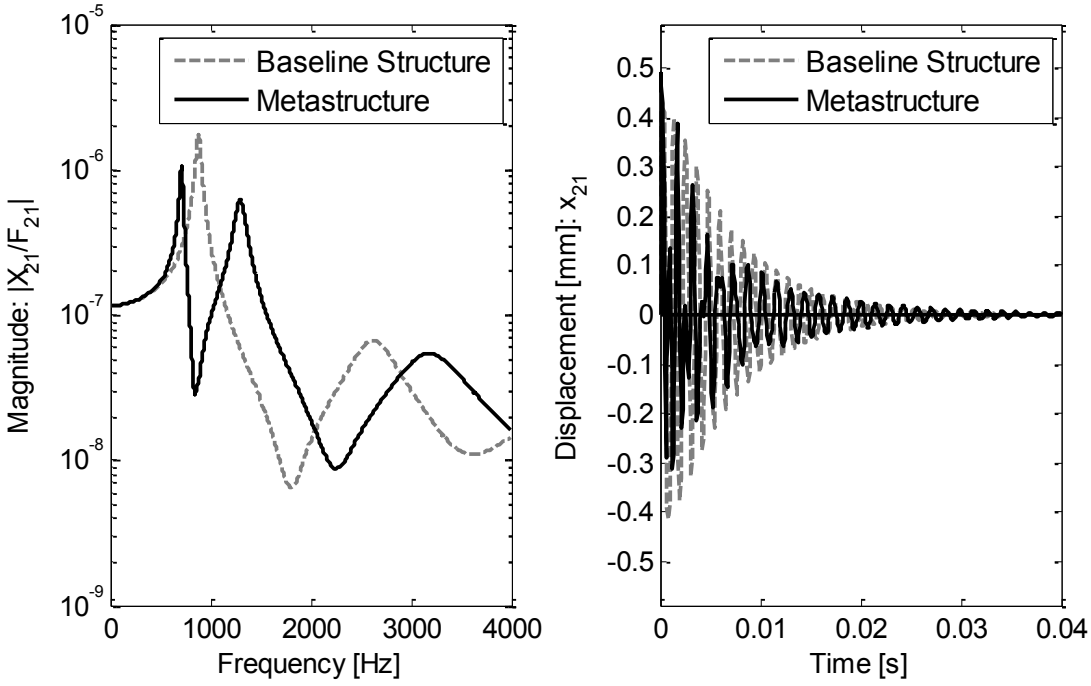

Fig. 4. FRF and Impulse Response of System with 20 absorbers with constant frequency

Simply increasing the number of absorbers while keeping the natural frequency the same for all absorbers does not make a significant impact, but it does allow for greater flexibility in the tuning of the parameters. From the previous results, the frequency at which the absorbers were tuned causes a dip in the FRF at that frequency. Instead of setting all the absorbers to a single frequency and getting one large dip, the next case tunes the absorbers to varying frequencies ranging from 500 to 1500 Hz in an effort to smooth out the peak instead of simply splitting the peak. The results displayed in Fig. 5 show that this produces favorable results. The peak is smoothed out and the H_2 norm has a decrease of 50.3%. In the impulse response function, the magnitude of the vibrations is also greatly reduced. Towards the end of the impulse response, beating phenomenon becomes apparent. Beating behavior occurs when there are closely spaced natural frequencies causing the amplitude of the impulse response to increase for a short period of time. Even with the increased levels due to beating, the displacement levels remain below the baseline model. In a zoomed version of the FRF, shown in Fig. 6, the closely spaced peaks are visible. The inverse of difference between the peaks corresponds to the time period of the beat seen in the time response.

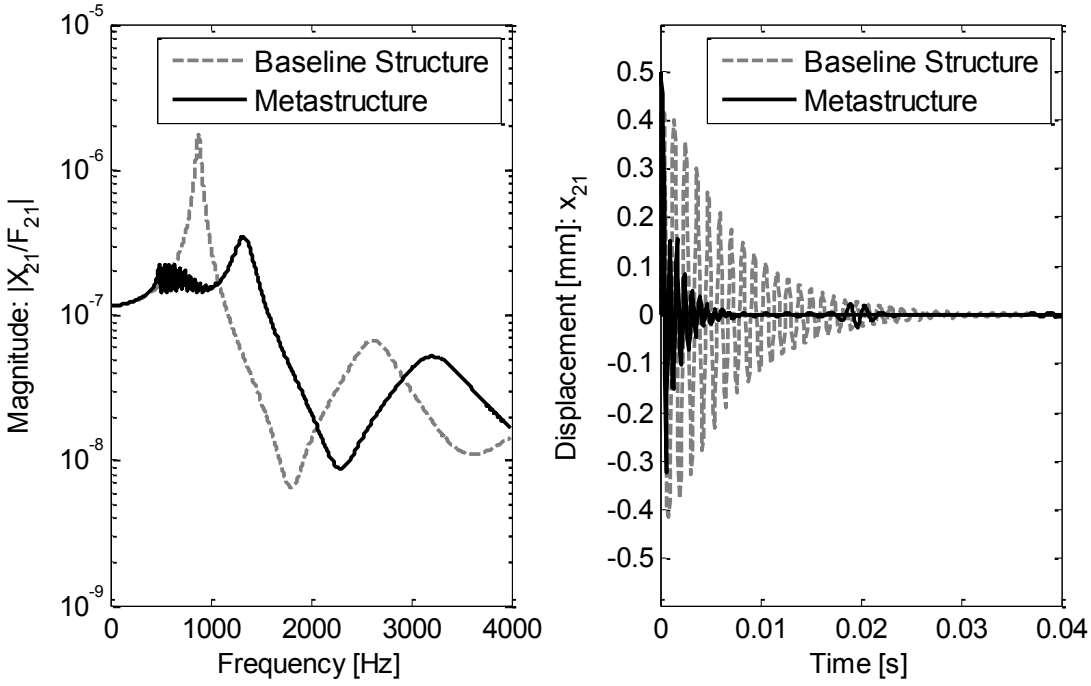

Fig. 5. FRF and Impulse Response of a Structure with 20 absorbers with linearly varying frequencies

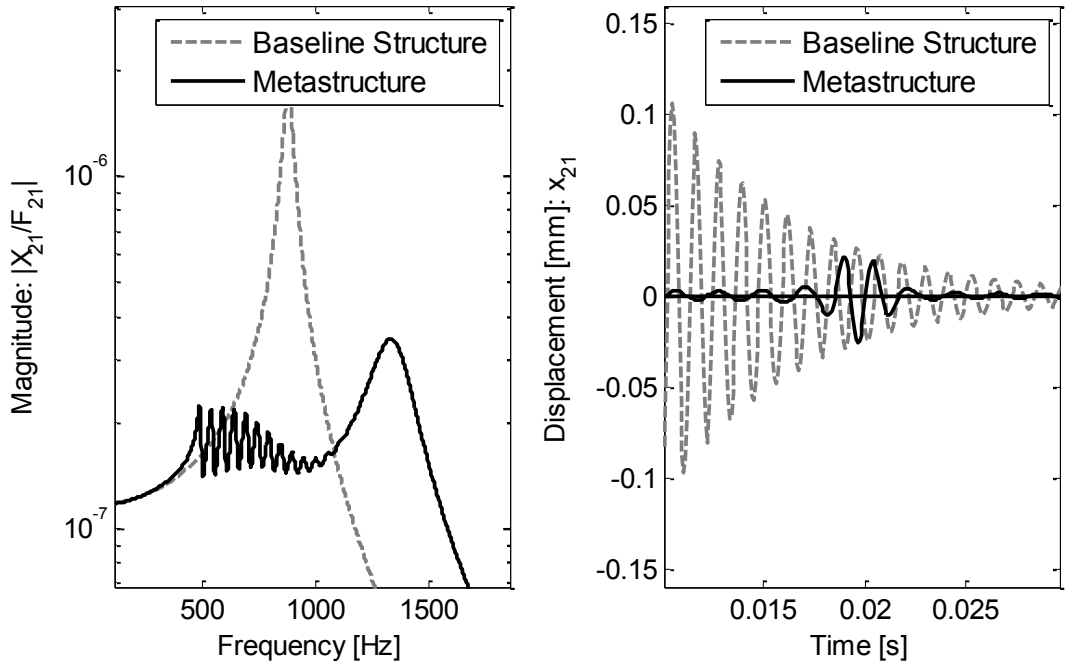

Fig. 6. Close-up View of Beating Behavior

5. Optimization

Next, an optimized version of this model is examined using a similar procedure to that of Zou and Nayfeh, who applied their methods to multiple degree of freedom tuned mass dampers [18]. Zou and Nayfeh optimized their model by minimizing the H_2 norm. A similar approach is taken in this model, but will maximize the percent decrease in the H_2 norm from the baseline structure to the metastructure. The negative of this percentage is used as the objective function and is minimized. The optimization is performed in MATLAB using a constrained non-linear interior point algorithm (`fmincon`). When the optimization is performed, the number of vibration absorbers is constrained to a single value and the algorithm determines the optimal values of the frequency range and mass ratio. The number of absorbers was not used as a parameter of the optimization since it does not take an optimal value. More absorbers lead to higher performance but also lead to a more complex structure. The complexity of a structure is difficult to quantity. This trade-off between performance and complexity is described in more detail in Section 6.3. When this optimization procedure is applied to the system with 20 absorbers from Section 4, the optimal range of frequencies is calculated as 513 – 2208 Hz and the optimal mass ratio is $\mu = 0.34$. The frequency range deviates slightly from the range estimated in Section 4, 500 – 1500 Hz and the mass ratio increases slightly from the estimated value of $\mu = 0.30$These new values used in the optimized model result in a 57.1% reduction in the H_2 norm, which is a greater reduction compared to the non-optimized model; see Table 2. The FRF and impulse response can be seen in Fig. 7.

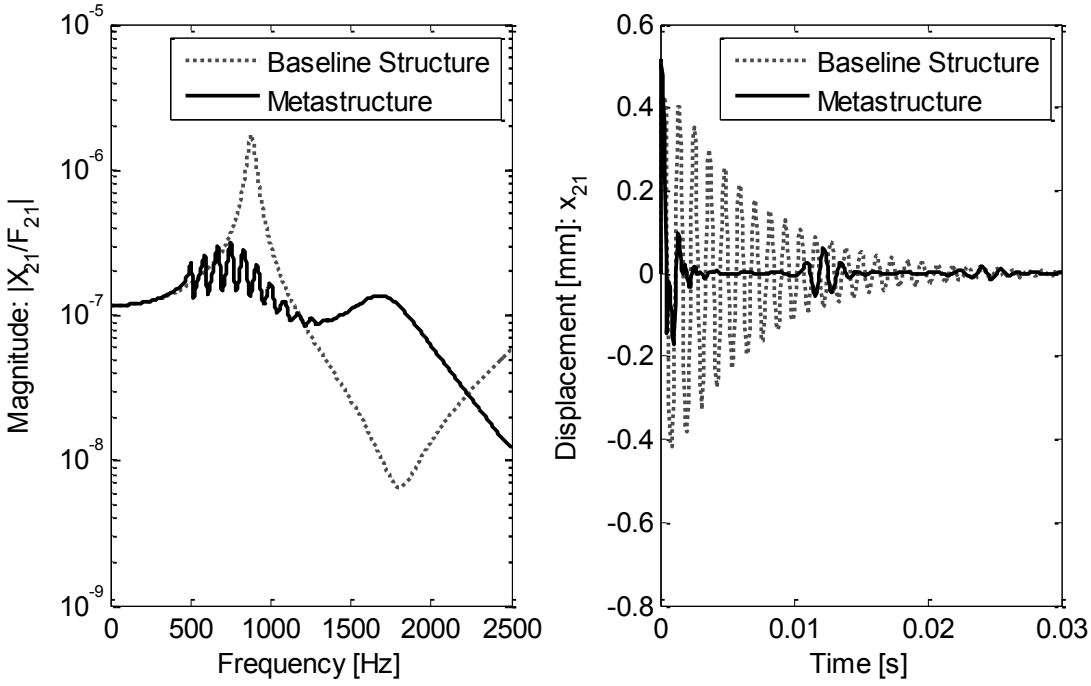

Fig. 7. Optimized Model for 20 absorbers

6. Parameters to Vary

A variety of parameters are examined, to see what the model is capable of and to help understand any basic phenomenon. This section explores the various parameters of the models to see how to get the best response in terms of the performance measures defined in the sections below.

6.1. Distribution of the Stiffness

As shown previously, the models in which the absorbers are tuned to frequencies that vary linearly provide better performance than those that are all tuned to a single frequency. Next, other distributions are examined. Instead of constraining the distribution to be linear, the optimization code allows each absorber to take on any value for its natural frequency. Fig. 8 shows the optimal distribution for a structure with 20 absorbers alongside the distributions for the linear and constant cases. The x-axis denotes the absorber number, ranging from 1 to n and the y-axis shows the natural frequency of that absorber. It is interesting to note the pattern of the optimal distribution, but it must also be noted that transitioning from the linear to the unconstrained distribution produces less than a 2% additional decrease. The decrease goes from 56.9% to 58.2%. The results are summarized in Table 2. This is deemed not beneficial enough to

outweigh the extra time it takes the optimization code to run. For the following analyses, a linear distribution is utilized.

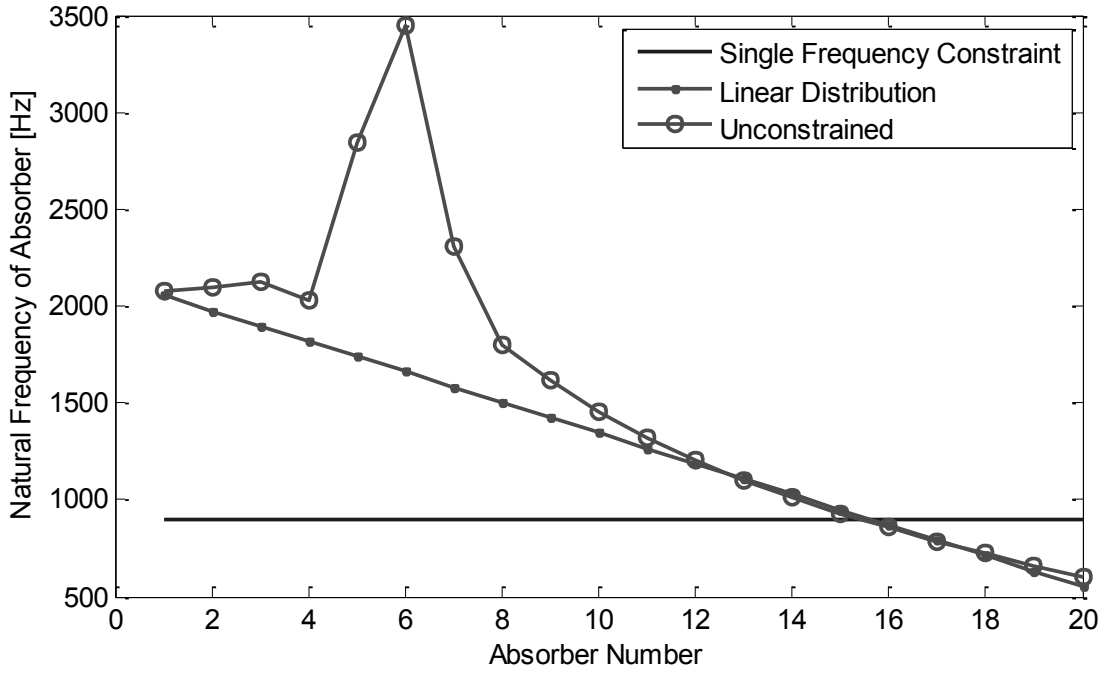

Fig. 8. Natural Frequeny of Indiviadual Vibration Absorbers

Table 2
Summary of Results from Various Configurations

	Number of Absorbers, $\boldsymbol{n}$	Absorber Frequency Range (Hz)	Percent Decrease in $\boldsymbol{H_2}$ Norm
Set to baseline fundamental frequency	2	766	26.0%
Set to baseline fundamental frequency	20	877	27.9%
Set to vary around baseline frequency	20	500 – 1500	50.3%
Optimized with respect to the H_2 norm (stiffness varies linearly)	20	513 – 2202	57.1%
Optimized with respect to the H_2 norm (no constraint set of stiffness distribution)	20	533 – 3420	58.2%

6.2. Mass Ratio

Next, the effect of the mass ratio on the system is determined. The mass ratio is included in the optimization procedure described in Section 5 but looking at the effects of varying the mass ratio provides insight into the behavior of the system. Recall, the definition of the mass ratio is the ratio of the mass of the absorbers over the mass of the host structure, Eq. (1). Once a mass ratio and a total mass is defined, the mass of the absorbers can be calculated; see Eq. (3) for details. Next, a optimization procedure similar

to the one described above is used to calculate the stiffness values of the absorber springs. For each data point in Fig. 9, the number of absorbers is set to 20, the mass ratio is varied, and the optimization procedure is performed. The resulting percent decrease is plotted and the shape of the plot shows there is an optimal mass ratio value which is why the mass ratio was added to the optimization procedure in Section 5. The existence of an optimal mass value show that there is a tradeoff between mass in the absorber system and mass in the host structure. Too little mass in the absorber system does not allow sufficient energy transfer to the absorber mass and too much mass produces a large response from a higher mode. From these results, a mass ratio of $\mu = 0.34$ is optimal for this specific structure. Fig. 10 shows the resulting FRF for four of the mass ratios.

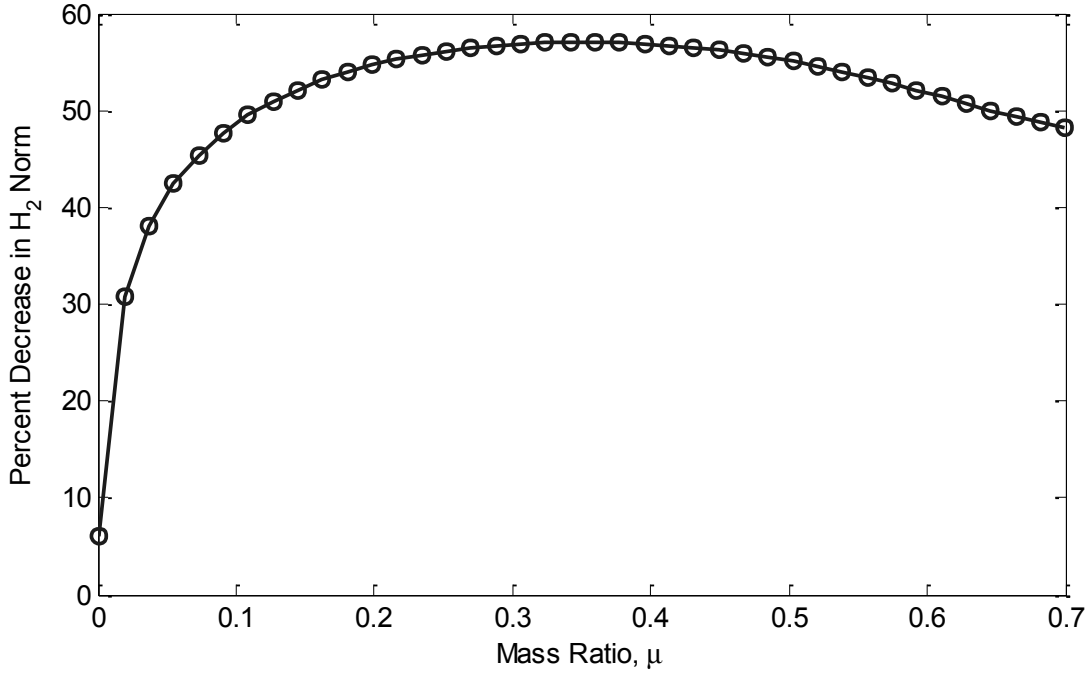

Fig. 9. Optimal Percent Decrease in $\boldsymbol{H_2}$ Norm for Varying Mass Ratios

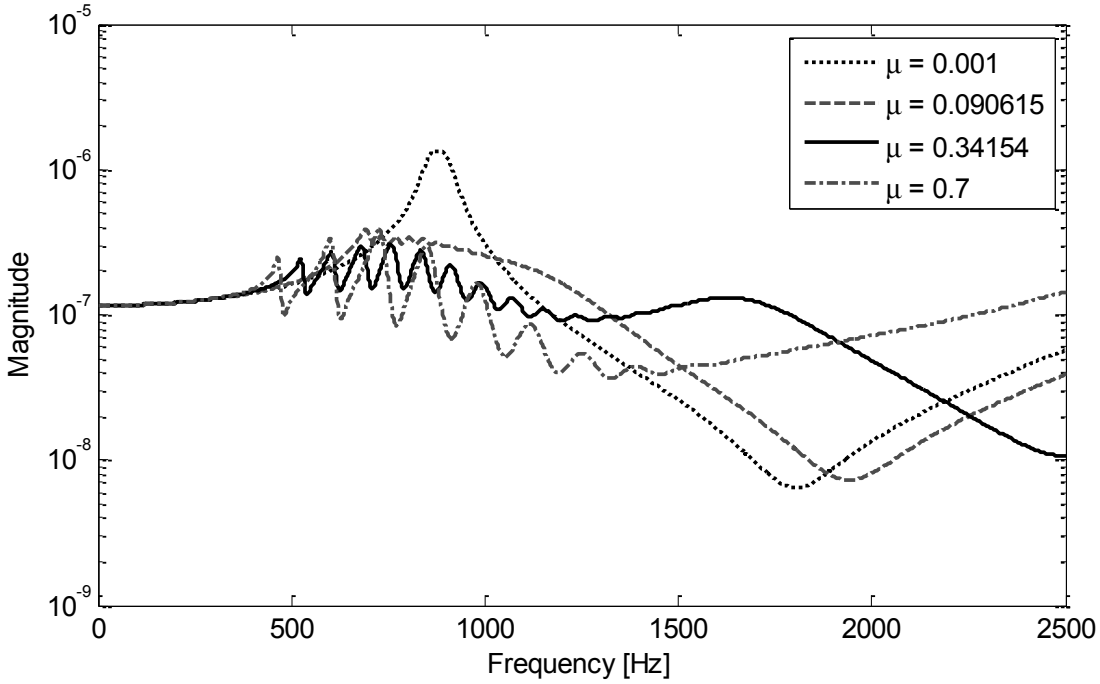

Fig. 10. Optimal FRFs for Various Mass Ratios

6.3. Number of Absorbers

Similar to above, the number of absorbers is also examined. An optimization procedure is run for each data point shown in Fig. 11. The results show there is not an optimal number of absorbers, but the performance tends towards an asymptote. The response improves as more absorbers are used, but at some point there is a trade-off between increased performance and increased complexity. For this paper, 20 absorbers is chosen because any structure with more than 20 absorbers provides only marginally better performance. The FRFs for systems with 2, 26, and 50 absorbers are plotted in Fig. 12.

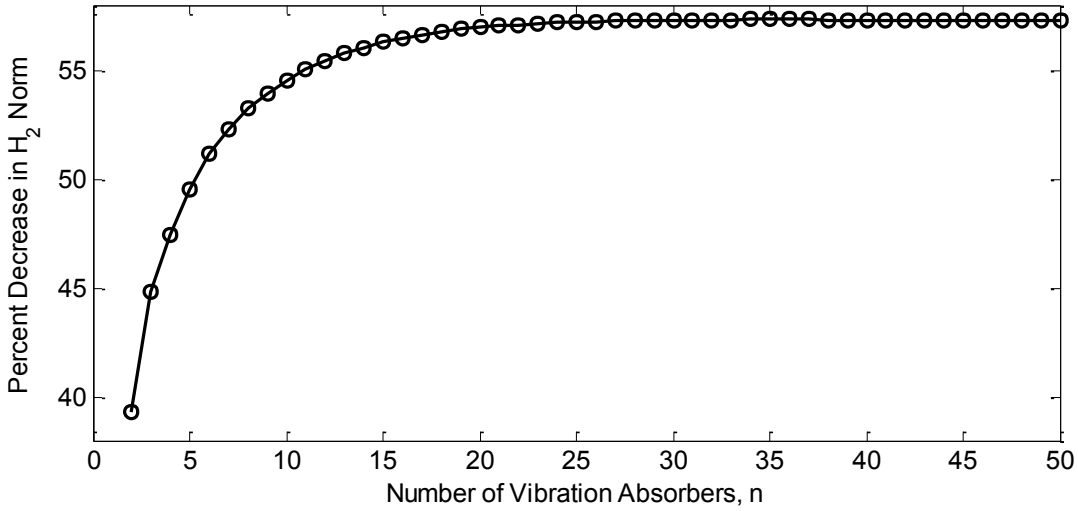

Fig. 11. Optimal Percent Decrease in $\boldsymbol{H_2}$ Norm for Varying Number of Absorbers

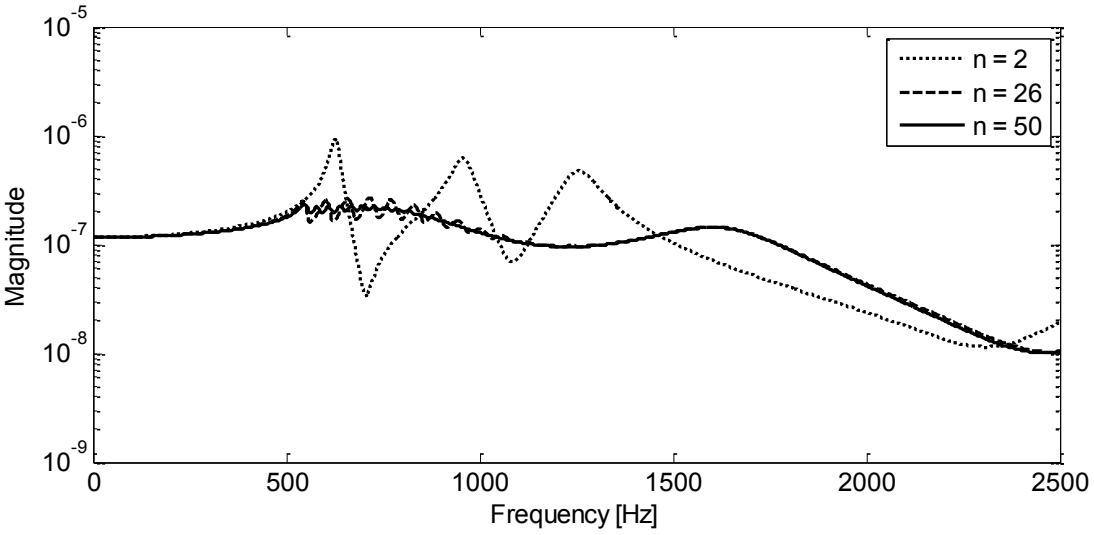

Fig. 12. Optimal FRFs for Various Number of Absorbers

7. Experimental and Finite Element Trend Verification

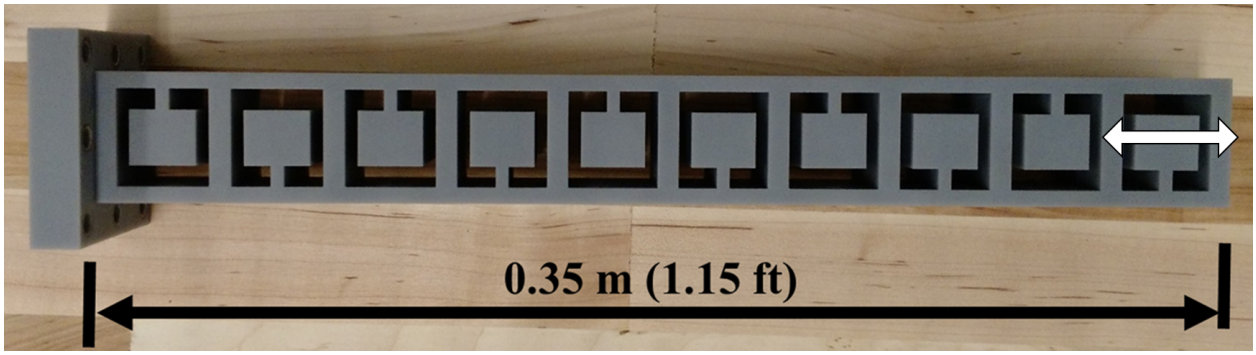

Fig. 13. Experimental Prototype Tested (arrow indicates direction or vibrations)

Experimental and finite element results are used to show that this model is accurately able to capture the effects of the metastructure but not to experimentally verify the model.The experimental results are taken from previously published work [25]. The metastructure is fabricated using 3D printing technologies and constructed from a single uniform material, shown in Fig. 13. As with the model presented in this paper, the structure was designed for vibration suppression in the longitudinal direction. There are ten absorbers distributed along the length of the beam, $n = 10$. The absorbers consist of a large mass with a cantilever beam used as the absorber spring. The cantilever beams are arranged in an alternative fashion to preserve symmetry during testing. In this structure all of the absorbers are identical. These experimental results are compared to the lumped mass model discussed in this work and to a 2D finite element model created in ANSYS. The method to calculate the model parameters from Section 2.1 is not used here. Instead, the model parameters are calculated based on the geometry of the physical structure. The methods of Section 2.2 are then utilized using the new parameters. The purpose of these comparisons is to show the experimental trends match the experimental trends. The lumped mass model does not accurately capture the dynamics of the real structure since it is a distributed system. But, it is important to recognize that the trends captured by the lumped mass model are trends seen in experimental results.

7.1. Experimental Results

Experimental testing was performed by Hobeck *et al* and is described in their paper, but a brief summary is provided here for completeness. Two conditions were tested; the free and blocked conditions, which are referred to as the metastructure and baseline structure here. The metastructure, or the free condition, allows the absorbers to vibrate freely, whereas the baseline structure, or the blocked configuration, has foam blocks which prevent the absorbers from moving. Both of these configurations have the same mass,

since the foam blocks have a mass which is small enough to be neglected. Two accelerometers were attached to the structure; one at the tip and one at base, and the structure was excited with an impulse by hitting the table with a hammer. Results from these experiments are shown in Fig. 14.

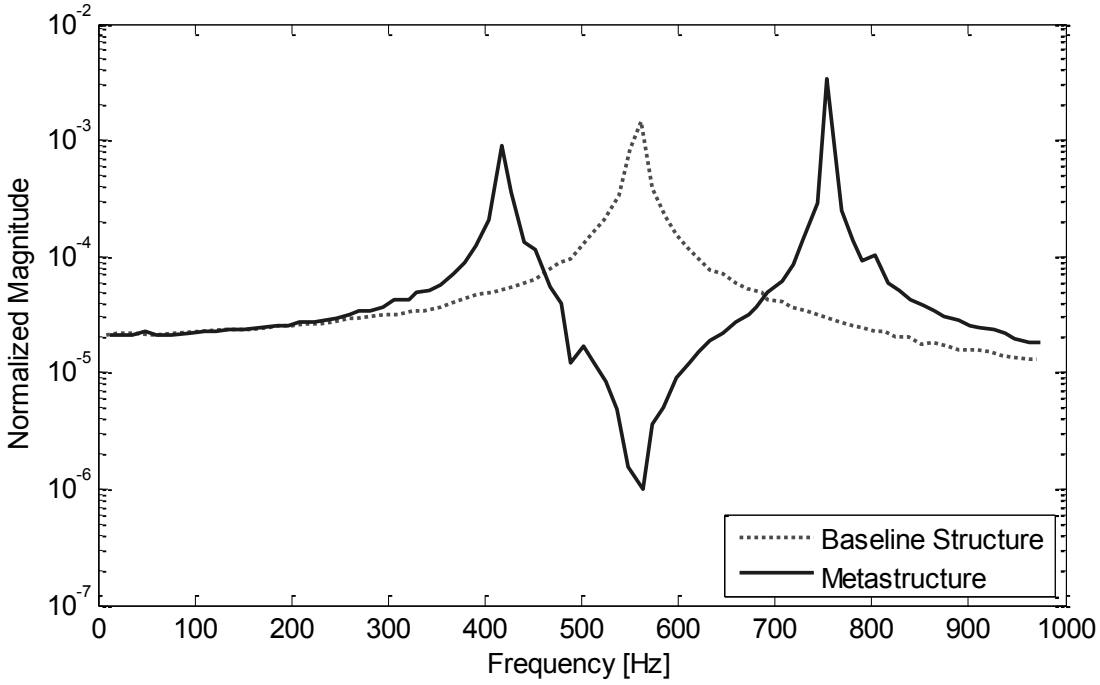

Fig. 14. Frequency Reponses Function of Experimental Results

7.2. Lumped Mass Model

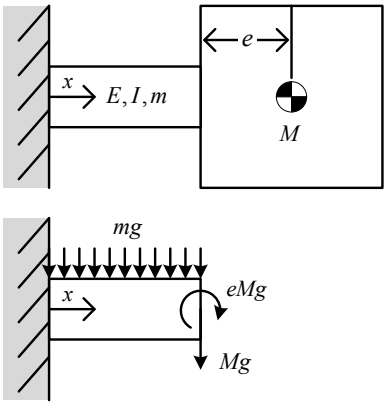

Fig. 15. Schematic of absorber

An analytical model in [25] was developed to estimate the absorber natural frequency. They used Rayleigh's quotient to determine the absorber natural frequency. The rest of the structure was modeled as a single degree of freedom system using basic lumped parameter assumptions. Their modeling methods will be modified such that the, previously described, multiple degree of freedom lumped mass model can be utilized. Modeling the absorbers is completed in a similar manner to Hobeck *et al*, using Rayleigh's quotient for a cantilever beam with a large tip mass. The assumed fundamental mode shape used is that of a cantilever beam undergoing uniform gravitational load with an applied tip shear and moment as seen in Fig. 15, and takes the following form

$$\phi = \frac{mg}{24EI}(x^2 + 6L^2 - 4Lx) + \frac{Mgx^2}{6EL}(3L - x) + \frac{Mgex^2}{2EI} \tag{17}$$

where m is the mass per unit length of the beam, g is the acceleration due to gravity, E is the Young's modulus of the material, I is the moment of inertia of the beam cross section, L is the length of the beam, x denotes the position along the beam ranging from 0 to L, M is the mass of the tip mass, and e is the distance from the tip of the beam to the center of mass of the tip mass. Using this assumed mode shape, the kinetic and potential energy of the system is calculated and the ratio of the energies provides an estimate of the fundamental natural frequency of the absorber, ω_a as

$$\omega_a^2 = \frac{\frac{1}{2}\int_0^L EI(\phi'')^2 dx}{\frac{1}{2}\int_0^L m\phi^2 dx + \frac{1}{2}M(\phi_L + e\phi_L')^2 + \frac{1}{2}J(\phi_L')^2} \tag{18}$$

where J is the polar moment of inertia of the tip mass, the prime $(\cdot)'$ indicates the derivative with respect to x, and the L subscript refers to the value of ϕ at the tip of the beam, *i.e.* $\phi_L = \phi(x = L)$.

The lumped mass model requires the mass and stiffness of the absorber. Since the experimental model is uniform, $k_1 = k_2 = \cdots = k_{10} = k_a$ and $m_1 = m_2 = \cdots = m_{10} = m_a$ The mass of the absorber, m_a can be determined from geometry and material properties. Then the effective stiffness, k_a is calculated as

$$k_a = m_a\omega_a^2 \tag{19}$$

The host structure parameters are calculated based on the geometry and material properties of the physical structure. The host mass, m_0, accounts for the mass of all the material that is not a part of the absorbers. The host spring stiffness is calculated as

$$k_0 = \frac{EA}{\ell} \tag{20}$$

where E is the Young's modulus of the material, A is the cross-sectional area, and ℓ is the distance between the host masses. These parameters are then used to determine the mass, stiffness, and damping matrices as described in Section 2.2. The results can be seen in Fig. 16. Only the metastructure is plotted because the baseline structure used earlier in this paper is fundamentally different than the one experimentally tested.

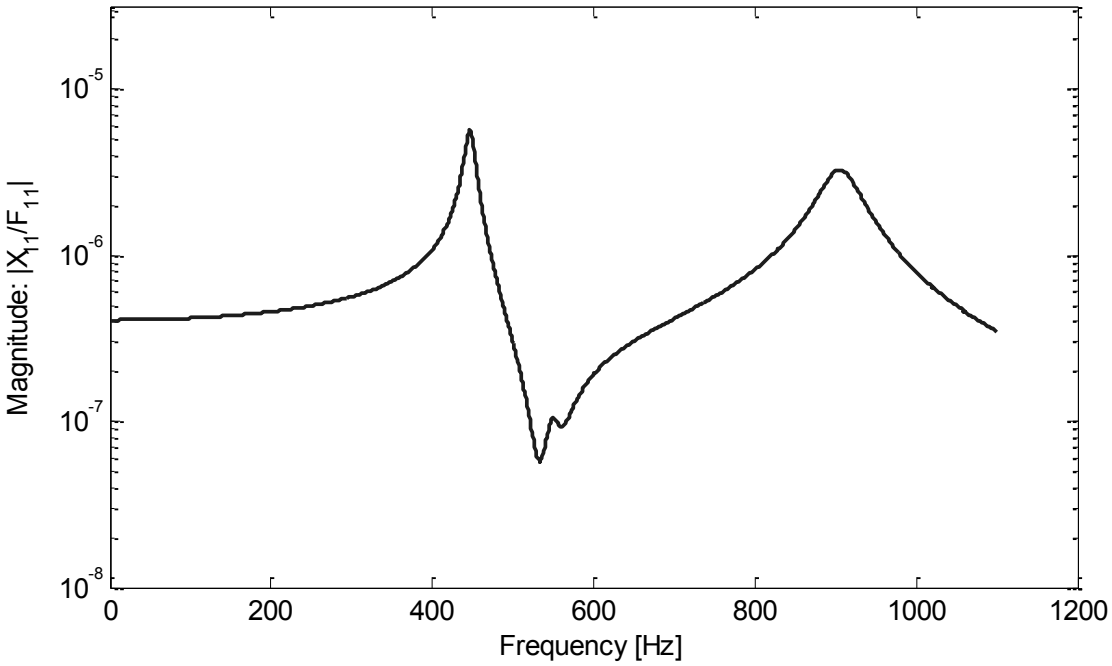

Fig. 16. Frequency Response Function of Lumped Mass Model

7.3. Finite Element

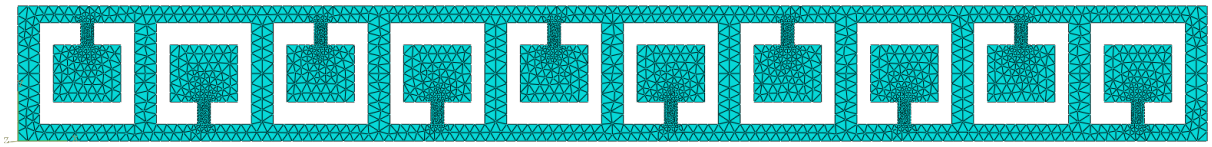

Fig. 17. 2D Finite Element Model of Metastructure

As a second verification, a finite element model of the structure is created in ANSYS. A 2D model is utilized to capture the bending effects of the absorbers without getting out of plane effects. The geometry and a mesh of the structure are shown in Fig. 17. The displacements and rotation of the model are constrained on the far left edge of the model and along the center of the structure. Excluding the absorbers, the model is only allowed to move in the longitudinal direction. This second constraint eliminates the in-plane bending modes, which are not of interest in the present work. A cyclic force is

applied to the far right side of the beam and the resulting displacement was measured and plotted in Fig. 18. The baseline model is created by adding massless, rigid blocks to the end of each absorber to prevent the absorbers from resonating emulating the experimental configuration.

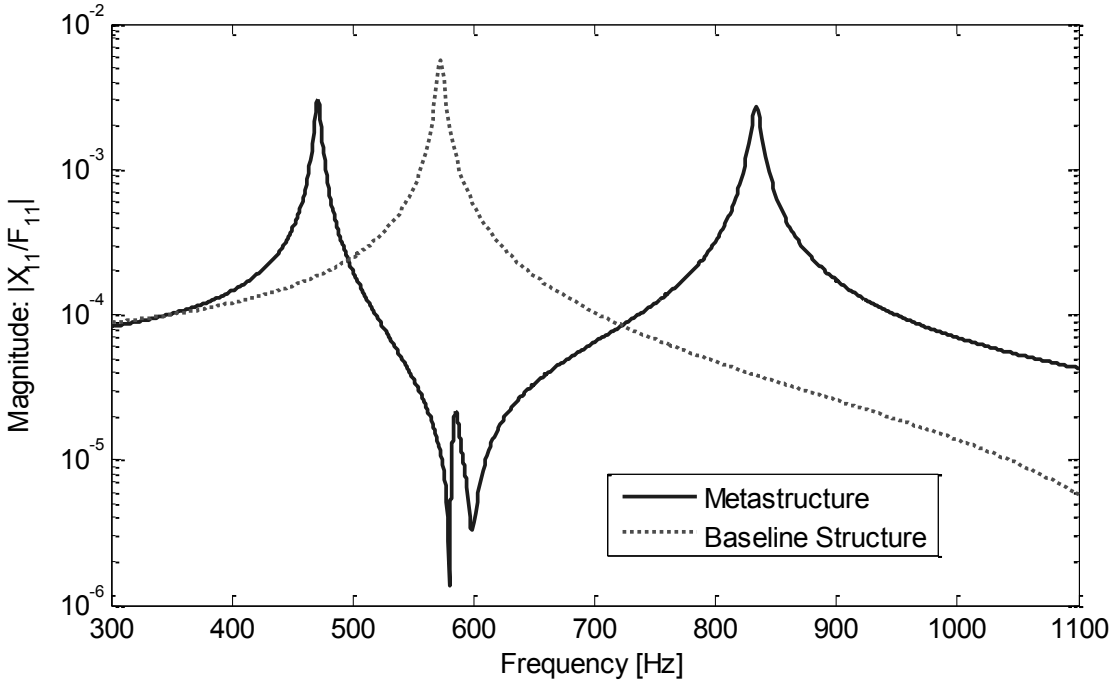

Fig. 18. Frequency Response Function of Finite Element Model

7.4. Comparison

Examining the results from the three different models, it is clear that each model captures the main effects of metastructure, namely that absorbers tuned to the natural frequency of the baseline structure are able to create a band gap where the baseline fundamental frequency occurs. The values of the various mode shapes and the percent errors are summarized in Table 3. These results agree reasonably well. The finite element model discrepancies can be accounted for due to the lack of precise knowledge of the Young's modulus of the printed material. Typically, these values are reported as a range of values. The lumped mass model has considerably more error in the 2nd mode. This is likely due to the fact that the mass of the experimental prototype is not lumped, but is relatively evenly distributed across the length of the bar. Thus, treating it as lumped masses introduces some error. Most importantly, this shows that the lumped mass model does exhibit realistic behavior that can also been seen in experimental studies.

Based on the results of this paper, the structure used by Hobeck *et al* [25] is not the optimal structure. The mass ratio they used, $\mu = 0.64$, is much higher than that shown to be optimal. Additionally, the results of this paper show that absorbers with varying natural frequencies perform better than structures with a single natural frequency.

Table 3
Table of Results from Experiment, Lumped Mass Model and Finite Element Model

	Baseline Structure		Metastructure			
	1st Mode [Hz]	Percent Error	1st Mode [Hz]	Percent Error	2nd Mode [Hz]	Percent Error
Experimental Results	560.5	-	417.3	-	754.0	-
Lumped Mass Model	-	-	446.1	6.90%	905.5	20.09%
Finite Element Model	572.6	2.16%	470.2	12.68%	832.2	10.37%

8. Conclusions

The results of these simulations show that it is possible to use distributed vibration absorbers to reduce the response of a system without adding additional mass to the structure. These simulations found that the distributed absorbers should be designed such that their natural frequencies span a range of frequencies. For this specific structure, the results show that the mass ratio (mass of the absorbers over the mass of the host structure) should be around 0.3 and the number of absorbers should be around 20. The natural frequencies of the vibration absorbers should be tuned such that their frequencies vary linearly. This set of parameters produces the most significant reduction in vibrations.

Acknowledgement

This work is supported in part by the US Air Force Office of Scientific Research under the grant number FA9550-14-1-0246 ‘’Electronic Damping in Multifunctional Material Systems’’ monitored by Dr. BL Lee and in part by the University of Michigan.

References

[1] S. Laszlo, E. Shamonina, A historical review, in: Waves in Metamaterials, 2009: pp. 315–324.

[2] N. Engheta, R.W. Ziolkowski, Metamaterials: Physics and Engineering Explorations, IEEE, 2006.

[3] S.A. Cummer, J. Christensen, A. Alù, Controlling sound with acoustic metamaterials, Nat. Rev. Mater. 1 (2016) 16001. doi:10.1038/natrevmats.2016.1.

[4] R. Martínez-Sala, J. Sancho, J. V Sánchez, V. Gómez, J. Llinares, F. Meseguer, Sound attenuation by sculpture, Nature. 378 (1995) 241–241. doi:10.1038/378241a0.

[5] M.I. Hussein, M.J. Leamy, M. Ruzzene, Dynamics of Phononic Materials and Structures: Historical Origins, Recent Progress, and Future Outlook, Appl. Mech. Rev. 66 (2014) 040802. doi:10.1115/1.4026911.

[6] G.W. Milton, J.R. Willis, On modifications of Newton's second law and linear continuum elastodynamics, Proc. R. Soc. A Math. Phys. Eng. Sci. 463 (2007) 855–880. doi:10.1098/rspa.2006.1795.

[7] Z. Liu, X. Zhang, Y. Mao, Y.Y. Zhu, Z. Yang, C.T. Chan, P. Sheng, Locally Resonant Sonic Materials, Science (80-.). 289 (2000) 1734–1736. doi:10.1126/science.289.5485.1734.

[8] R. Zhu, X.N. Liu, G.K. Hu, F.G. Yuan, G.L. Huang, Microstructural designs of plate-type elastic metamaterial and their potential applications: a review., Int. J. Smart Nano Mater. 6 (2015) 14–40. doi:10.1080/19475411.2015.1025249.

[9] K.K. Saxena, R. Das, E.P. Calius, Three Decades of Auxetics Research − Materials with Negative Poisson's Ratio: A Review, Adv. Eng. Mater. (2016) 1–24. doi:10.1002/adem.201600053.

[10] H. Sun, X. Du, P.F. Pai, Theory of Metamaterial Beams for Broadband Vibration Absorption, J. Intell. Mater. Syst. Struct. 21 (2010) 1085–1101. doi:10.1177/1045389X10375637.

[11] P.F. Pai, Metamaterial-based Broadband Elastic Wave Absorber, J. Intell. Mater. Syst. Struct. 21 (2010) 517–528. doi:10.1177/1045389X09359436.

[12] T. Igusa, K. Xu, Wide-Band Response of Multiple Subsystems with High Modal Density, in: 2nd Int. Conf. Stoch. Struct. Dyn., 1990: pp. 131–145.

[13] T. Igusa, K. Xu, Vibration Control Using Multiple Tuned Mass Dampers, J. Sound Vib. 175 (1994) 491–503. doi:10.1006/jsvi.1994.1341.

[14] H. Yamaguchi, N. Harnpornchai, Fundamental Characteristics of Multiple Tuned Mass Dampers for Supressing Harmonically Forced Oscillations, Earthq. Eng. Struct. Dyn. 22 (1993) 51–62.

[15] J.P. DenHartog, Mechanical Vibrations, McGraw-Hill, New York, 1947.

[16] J.Q. Sun, M.R. Jolly, M.A. Norris, Passive, Adaptive and Active Tuned Vibration Absorbers—A Survey, J. Vib. Acoust. 117 (1995) 234 – 242. doi:10.1115/1.2838668.

[17] N. Hoang, P. Warnitchai, Design of multiple tuned mass dampers by using a numerical optimizer, Earthq. Eng. Struct. Dyn. 34 (2005) 125–144. doi:10.1002/eqe.413.

[18] L. Zuo, S.A. Nayfeh, Minimax optimization of multi-degree-of-freedom tuned-mass dampers, J. Sound Vib. 272 (2004) 893–908. doi:10.1016/S0022-460X(03)00500-5.

[19] Y. Xiao, J. Wen, X. Wen, Longitudinal wave band gaps in metamaterial-based elastic rods containing multi-degree-of-freedom resonators, New J. Phys. 14 (2012). doi:10.1088/1367-2630/14/3/033042.

[20] Y. Shanshan, Z. Xiaoming, H. Gengkai, Experimental study on negative effective mass in a 1D mass-spring system, New J. Phys. 10 (2008) 0–11. doi:10.1088/1367-2630/10/4/043020.

[21] H.H. Huang, C.T. Sun, G.L. Huang, On the negative effective mass density in acoustic metamaterials, Int. J. Eng. Sci. 47 (2009) 610–617. doi:10.1016/j.ijengsci.2008.12.007.

[22] R. Zhu, G.L. Huang, H.H. Huang, C.T. Sun, Experimental and numerical study of guided wave propagation in a thin metamaterial plate, Phys. Lett. A. 375 (2011) 2863–2867. doi:10.1016/j.physleta.2011.06.006.

[23] G. Wang, X.S. Wen, J.H. Wen, Y.Z. Liu, Quasi-One-Dimensional Periodic Structure with Locally Resonant Band Gap, J. Appl. Mech. 73 (2006) 167–170. doi:10.1115/1.2061947.

[24] A. Qureshi, B. Li, K.T. Tan, Numerical investigation of band gaps in 3D printed cantilever-in-mass metamaterials, Sci. Rep. 6 (2016) 1–10. doi:10.1038/srep28314.

[25] J.D. Hobeck, C.M. V Laurant, D.J. Inman, 3D Printing of Metastructures for Passive Broadband Vibration Suppression, in: 20th Int. Conf. Compos. Mater., Copenhagen, 2015.

[26] E.D. Nobrega, F. Gautier, A. Pelat, J.M.C. Dos Santos, Vibration band gaps for elastic metamaterial rods using wave finite element method, Mech. Syst. Signal Process. 79 (2016) 192–202. doi:10.1016/j.ymssp.2016.02.059.

[27] O. Abdeljaber, O. Avci, D.J. Inman, Optimization of chiral lattice based metastructures for broadband vibration suppression using genetic algorithms, J. Sound Vib. 369 (2015) 50–62. doi:10.1016/j.jsv.2015.11.048.

[28] T. Yu, G.A. Lesieutre, Damping of Sandwich Panels via Acoustic Metamaterials, in: AIAA SciTech, 57th AIAA/ASCE/AHS/ASC Struct. Struct. Dyn. Mater. Conf., 2016.

[29] C. Claeys, E. Deckers, B. Pluymers, W. Desmet, A lightweight vibro-acoustic metamaterial demonstrator: Numerical and experimental investigation, Mech. Syst. Signal Process. 70-71 (2015) 853–880. doi:10.1016/j.ymssp.2015.08.029.

[30] A.M. Kabe, B.H. Sako, Issues with Proportional Damping, AIAA J. 54 (2016) 2864–2868. doi:10.2514/1.J054080.